Navigator 2007 – Centerfold – NAVO MSRC CAP II – Version 1.2.3.3 – Cleared for public release: VS07.005-129 Case No. ESC 07-0689.

Lattice model of fluid turbulence

Jeffrey Yepez[1], George Vahala[2], Linda Vahala[3], Min Soe[4], Sean Ziegeler[5]
[1]*Air Force Research Laboratory, Hanscom Air Force Base, MA 01731*
[2]*Department of Physics, William & Mary, Williamsburg, VA 23185*
[3]*Department of Electrical & Computer Engineering, Old Dominion University, Norfolk, VA 23529*
[4]*Department of Mathematics and Science, Rogers State University, Claremore, OK 74017*
[5]*High Performance Computing Modernization Program, Mississippi State University, MS 38677*

The kinetic lattice gas is an optimal model of a vast many-particle system (such as a fluid) with complicated particle-particle interactions and irregular boundary conditions. With it the fluid dynamicist can achieve higher nonlinearity (measured by Reynolds number), unconditional stability and accuracy, with less memory and processor time than with other models of turbulence for situations with tortuous boundaries. For an engineer, it is simple to code, runs perfectly on parallel supercomputers, and is suited to a plethora of computational physics applications. As demonstrated here, it is a competitive alternative to large eddy simulations with Smagorinsky sub-grid closure. To theorists and experimentalist in quantum information science, its kinetic transport equation is a special case of the quantum dynamics, particularly governing a parallel array of quantum processors, a type-II quantum computer architecture. Presented are turbulent fluid simulations using the kinetic lattice gas model carried out on the supercomputer Babbage. As an illustration of the efficiency of the lattice model, presented is a discovery of a universal range in the morphological evolution of the laminar-to-turbulent flow transition: the breaking subrange.

Keywords: kinetic lattice gas model, type II quantum computing, entropic lattice Boltzmann equation, fluid turbulence

I. INTRODUCTION

In the defense community there are a plethora of neutral-fluid flows problems, particularly flows by regions with non-trivial spatial boundaries, such around an aircraft fuselage or a ship hull, through a jet engine compartment, or over the Earth's surface. While analytical solutions to such problems remain elusive and generally intractable, today they are within the reach of the computational physicist. To tackle such problems, practitioners usually resort to direct numerical simulation methods, yet here the amount of computer memory and processing time grows faster that the number of desired computed field points. Even in cases with simple or periodic boundaries, where more efficient numerical representations are available (such as a psuedo spectral approach pioneered by G.I. Taylor in the 1930's and S.A. Orszag *et al.* in the 1970's [1]), the scaling of computer resources with grid size is daunting. This computational complexity has translated into significant annual costs to defense department high performance computing offices purchasing large numbers of processing elements (typically thousands or ten of thousands), configured in massive parallel computing arrays. But this cost, increasing year after year, has been borne so engineers can solve mission critical fluid problems, perpetually requiring higher resolution grids and more accurate and faithful simulations. For example, high resolution flow simulations are vital to aeronautical engineers designing the shape of advanced fighter jets or unmanned aerial vehicles or submarines to economize on fuel consumption and minimize maneuvering instabilities and wakes, to propulsion engineers designing nozzle and flow control orifices to maximize thrust, or to meteorologists trying to understand intermittent turbulence induced in the upper atmosphere under the jet stream to maximize laser propagation from airborne platforms. Yet to the theoretical physicist, the situation is even more dire: the prediction of any aspects of turbulence (beyond Kolmogorov's 1941 universality hypothesis), using advanced statistical methods and perturbation methods, borrowed from triumphant quantum field theory and statistical mechanics, remains the oldest and most prominent of classical grand challenge problems, open now for over 150 years.

This dire situation arises because, even in the macroscopic limit, strong correlations and feedback mechanisms between large scale and small scale flow structures, over many decades of spatial separation, dominate the overall flow evolution. The clearest high level picture capturing the essential physics of this problem, with restrictioned attention to divergence free and low Mach number flows, are the incompressible Navier-Stokes equations. The strong correlation between disparate scales is captured by the extremely simple non-local convective derivative (the second order nonlinearity in the velocity field).

II. LAMINAR TO TURBULENT FLOW TRANSITION

The lattice model now affords a deep insight into the origin and essential inner workings of free shear turbulence. This is a *kinetic lattice gas model*, the clearest low level picture correctly capturing the essential physics and hydrodynamics of the problem. As the well known Ising lattice gas model is fundamental to a statistical mechanics understanding of the essential physics of ferro-

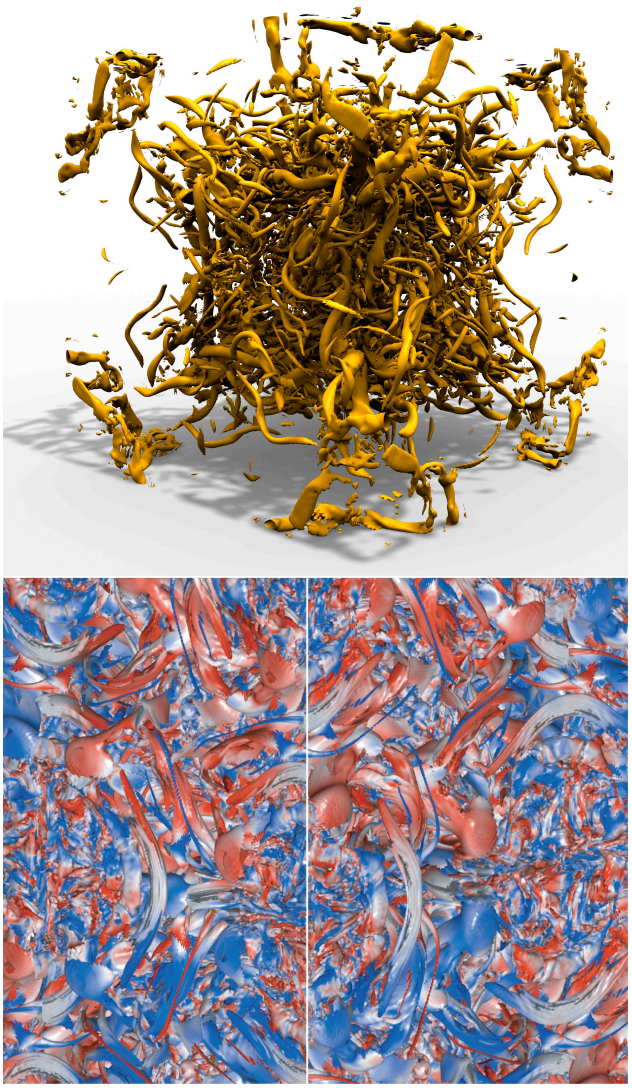

FIG. 1: Supercomputer simulation of Navier-Stokes turbulence. Surface of constant vorticity in turbulent flow, showing entangled vortex tubes (top) and anisotropic flow in the *breaking subrange* (bottom). The dot product of the velocity and vorticity fields are displayed in the red-blue color coding. The bottom image is a zoomed view of at $t = 5K\Delta t$ time step shown if Fig. 2, where the vertical white line is one edge of the cubical simulation grid. Long vortex tendrils are easily seen. Fig. 1 shows the fastest executing code for computational fluid dynamics simulations of turbulence to date. This was computed on the newest defense department supercomputer, BABBAGE, located at the Naval Oceanographic Office MSRC at the Stennis Space Center in Mississippi, through a Capability Application Program (CAP) II grant. Also tested were new sub-grid models of turbulence, using lattice Boltzmann equation techniques, an entropic method and a Smagorinsky closure method. These codes are close cousins to quantum algorithms for aerodynamics. Our CAP II simulations used over one million hours, using a dedicated block of thousands of high performance processors over the period of four weeks, generating terabytes of data per day. These large-scale simulations offer a better understanding of the morphological evolution and structural development of turbulence in fluids, but they also give a preview of the kind of numerical output to be available from future quantum computers.

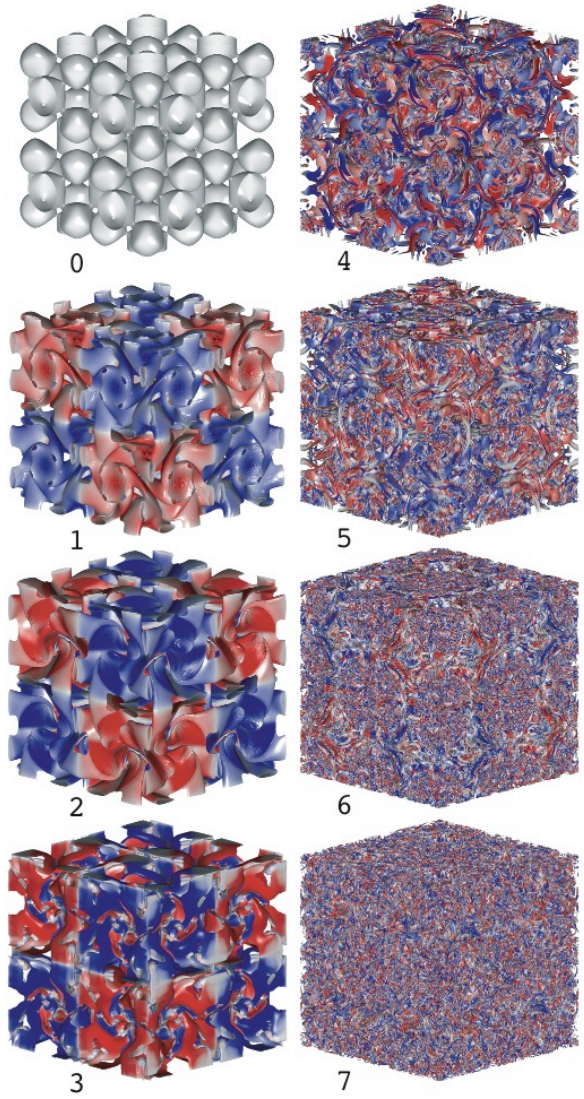

FIG. 2: Surfaces of constant enstrophy ($\mathscr{E} = \frac{1}{2}\int dV|\vec{\omega}|^2$ where $\vec{\omega} = \nabla \times \vec{u}$) illustrating an incompressible fluid's morphological evolution from $t = 0$ up to $t = 7,000\Delta t$ iterations, in time steps of $1,000\Delta t$ on a cubical cartesian grid of size $L = 512\Delta x$. Surface coloring uses $\vec{u} \cdot \vec{\omega}$ (red equals -1 and blue 1). This 3+1 dimensional turbulent neutral fluid simulation run was on the newest defense department supercomputer, BABBAGE, using the entropic lattice Boltzmann equation with 15-body particle-particle collisions (ELB-Q15 model) computed at every lattice site at each time step. At each site, local relaxation of the single-particle probability distribution a desired equilibrium function, represented as a low Mach number polynomial expansion. The initial flow is a Kida and Murakami profile [2] with a super cell size set to $L_\circ = 512\Delta x$, the total grid size. So the flow configurations within all 8 octants of the large grid are initially identical. The characteristic flow speed is $u_\circ = 0.07071\frac{\Delta x}{\Delta t}$. The collisional inversion parameter is set to $\beta = 0.99592$, corresponding to a kinematic viscosity of $\nu_\circ = 6.8 \times 10^{-4}\frac{\Delta x^2}{\Delta t}$, for $\alpha = 2$. The Reynolds number is $\mathrm{Re} = \frac{L_\circ u_\circ}{\nu_\circ} = 53,024$. The resulting turbulence is not fully resolved down to the dissipation scale, which in the model is the cell size Δx. Do do this, set $L = \mathrm{Re}^{\frac{3}{4}} \sim 2,078\Delta x$. So the flow is under resolved by about a factor of 4.

magnetism and the order-disorder phase transition, the kinetic lattice gas model is fundamental to a dynamical mechanics understanding of fluids and the laminar-to-turbulent flow transition. See Appendix A for a brief mathematical overview of the model.

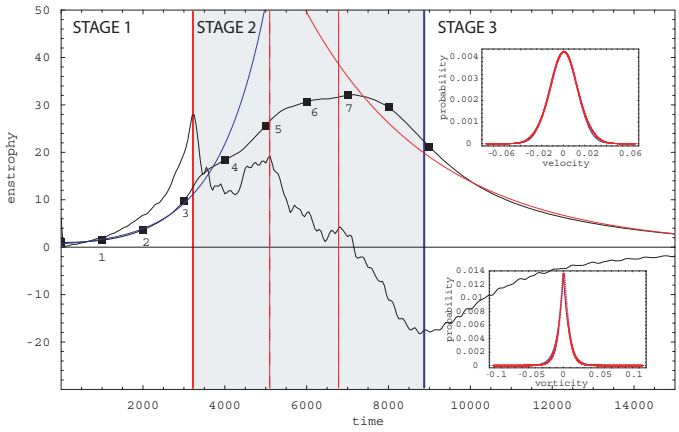

FIG. 3: Plot of enstrophy versus time (smooth black curve) showing three stages in the morphological evolution: (1) vortex stretching range ($t < 3,200\Delta t$), (2) breaking subrange ($3,200 < t < 9,000\Delta t$), and (3) inertial subrange ($t > 9,000\Delta t$). The enstrophy is normalized so that at $t = 0$ it is unity. The isovalues used to visualize the 8 images in Fig. 2 are shown (black squares). STAGE 1: The initial exponential increase (blue curve) of enstrophy designates the initial *vortex stretching range* with characteristic laminar flow. There is excellent agreement between the analytical fit (blue curve) and the enstrophy data (black curve). STAGE 2: The time derivative of the enstrophy curve (jagged black curve) is also plotted. The time period of generally negative slope of the enstrophy derivative (gray shaded region) is here termed the *breaking subrange*, where large scale anisotropic ordering of turbulence occurs and intermittently breaks down over time. The first major breaking point occurs at about $t = 3,200\Delta t$ (vertical red line) and subsequent intermediate avalanches occur at about $t = 5,100\Delta t$ and $t = 6,750\Delta t$ (thin vertical red lines), respectively. STAGE 3: The final exponential decrease of enstrophy (red curve) designates the *inertial subrange* where the homogeneous and isotropic "small scale" turbulent flow morphology, with characteristic entangled vortex tubes, is organized in a spatially self-similar way. Here the energy spectral density obeys the Kolmogorov universality hypothesis, the famous $k^{-\frac{5}{3}}$ power law for energy cascade downward to smaller scales. The onset of the inertial subrange occurs close to $t = 9,000\Delta t$ (vertical blue line). Here the velocity probability distribution functions, for each component, are Gaussian (top inset) and the vorticity probability distribution function approaches an exponential (bottom inset). There is excellent agreement between the analytical fit (blue curve) and the enstrophy data (black curve). There exists a fourth stage of the morphology of turbulence at late times ($t > 14,000\Delta t$), not shown here, called the *viscous subrange*.

A new universal feature of the laminar-to-turbulent transition becomes clear in high Reynolds number simulations. Following an initial period of laminar flow with vortex sheet stretching, and preceding the final inertial subrange period of isotropic and homogeneous turbulent flow with self-similar vortex tubes, there exists a well-defined interim period, here termed the *breaking subrange*. The hypothesis is that this subrange manifests self-organized criticality. The breaking subrange is dominated by anisotropic and non-homogeneous turbulent flow. Avalanches occur intermittently, where large coherent spatial structures grow, become unstable under maximal shear, and subsequently break into isotropic and homogeneous turbulence. These avalanches occur progressively in time across the entire space. See the bottom image of Fig. 1 showing the kind of anisotropic turbulent flow that occurs during an avalanche event, with young vortex tendrils. The time rate of change of the enstrophy, $\frac{\partial \mathscr{E}}{\partial t}$, has a generally negatively sloped avalanche cascade, with marked peaks, indicating the successive breaking points, as shown in Fig. 3.

By carefully comparing the renderings in Fig. 2 to the enstrophy plots in in Fig. 3, it is possible to see three distinct morphological stages of the flow: vortex stretching range, breaking subrange, and the inertial subrange. The morphological evolution transitions from (1) large vortex sheets to (2) convoluted vortex sheets with virgin vortex tendrils to (3) small entangled vortex tubes.

III. Q VERSUS S MODELS: CLOSURE OF SUB-GRID EFFECTS

The continuum hydrodynamical equations are projections of the entropic lattice Boltzmann (ELB) equation, a projection down from the $Q \times L^D$-dimensional kinetic phase space on to a $4 \times L^D$-dimensional hydrodynamic null space [1]. This projection recovers the Navier-Stokes equations in the Chapman-Enskog limit. This has an important consequence: there exist many "qubit" models (or Q models for short) with a different local stencils (*i.e.* lattice vectors sets with different finite point group symmetries and coordination number), which will also recover the Navier-Stokes equations asymptotically (continuous rotational symmetry).

ELB is ideal for large eddy simulation (LES) closures since in LES one typically deals with mean strain rates for modeling the eddy viscosity. These nonlocal fluid calculations are immediately recovered from simple local moments in ELB.

At this stage, the ELB runs are a validation of the method and this is important because ELB is a crucial precursor to a viable quantum lattice Boltzmann method [3]. The good numerical agreement between the LES-LB (lattice Boltzmann equation with sub-grid Smagorinsky closure here referred to as an S model) and the basic ELB Q models is encouraging. Now fully convinced of the validity of ELB, work to speed it up for present day supercomputer implementations is underway. But the most

[1] A subset of all the eigenvectors in the Q-dimensional kinetic space, have zero eigenvalues. These eigenvectors span the hydrodynamic null space. It is 4 dimensional because the kinetic lattice gas model conserves probability (mass) and probability flux along the spatially orthogonal directions (three components of the momentum vector).

promising opportunity is to simply build a type-II quantum computer [4, 5], which could far outstrip any classical supercomputers, for turbulence fluid simulations. In the fullness of time, the ELB will outpace the LES-LB, even without quantum computers.

There are a few reasons for this view. First, the kinetic lattice gases obey detail balance while sub-grid closure methods, such as the LES-LB, do not. And another advantage of the ELB over LES-LB is that ELB obeys the second law of thermodynamics while LES-LB and other LES methods do not necessarily obey the second law. Third, in the LES-LB the strain tensor must be computed at every site. With no-slip boundaries, computing the strain tensor becomes problematic. In contrast, ELB is purely local, so grid sites near boundaries are handled as easily as sites far away from boundaries. All these are important differences when the model is used for practical engineering grade applications.

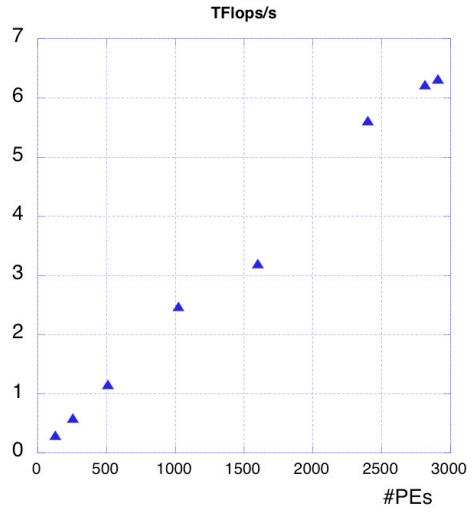

FIG. 4: TFlops/sec scaling of ELB-Q27 code on BABBAGE with number of CPUs.

IV. TIMINGS AND SCALING

Turbulent dynamics are easily solved since the underlying kinetic equation (A1) has only local algebraic nonlinearities in the macroscopic variables and simple linear advection. At this mesoscopic level there are various kinetic lattices (Q=15, 19, or 27) with different lattice vectors on a cubic lattice, which model the Navier-Stokes equation to leading order in the Chapman-Enskog perturbative asymptotics.

With the CAP data obtained on BABBAGE, the effects of the underlying lattice symmetry on the fluid turbulence statistics (through autocorrelation tensors of velocity, vorticity, pdfs of vorticity, and the like) can be determined, but there is not have sufficient space to present details here. The Q15 model seems to be the most efficient model. An example output of this model is shown in Fig. 2. Even on a relatively modest size 512^3 grid, we can achieve such a high degree of resolved nonlinearity (Re=26,512) that the consequent isotropic turbulence at the onset of the inertial subrange (at about $t \sim 9,000\Delta t$) outstrips the ability to visualize the myriad vortex tubes. Fig. 2 is just a test case. The sustained floating point per seconds (MFLOPS/PE) we achieved are the best of all scientific codes run, for example on the Earth Simulator, attaining over 67% of peak performance on 4,800 processors. Achieving the world's highest Reynolds number in the field of computational fluid dynamics should also occur in the near future. The current tested code on BABBAGE, on $1,600^3$ grid with 2,048 processing elements, can achieve a Reynold's number of Re=565,667. Modeling atmospheric scale turbulence, in the range of Re $\sim 10^6$ is possible today, for the first time in the half century long history of numerical digital computers applied to aerodynamics.

Some runs with these models–in particular the Q15, Q19, Q27 and S27 models–have been completed. The advantages of these lower Q models are reduced wall-clock times with less memory demands. The nonlinear convective derivatives of in the Navier-Stokes equation are recovered from purely local moments of kinetic space distribution function. This is the basic reason why ELB scales so well with PEs: the algorithm consists of simple local computations and streaming of information only to near neighbor grid sites.

No. PEs	GRID	MODEL	WALLCLOCK (s)	GFlops/s per PE
2912	1950^3	ELB-Q27	7,554.7	2.17
2912	1950^3	ELB-Q19	5,602.7	2.24
2912	1950^3	ELB-Q15	4,798.4	2.05
2912	1950^3	LES-LB-S27	4,451.2	1.05

TABLE I: The gigaflops per second per processor element for 2912 CPU runs on a $1952 \times 1946 \times 1950$ grid for four lattice Boltzmann codes variants. The wallclock time is for $2{,}000\Delta t$ (lattice time steps). A full turbulence simulation takes about 54,000 time steps.

During Phase I, investigating the scaling properties of the Q27 code, over 6.3 tera flops per second on the full 2912 processor elements available on BABBAGE was achieved, see Fig. 4.

The LES-LB-S27 code, which no longer needs the solution of an entropy constraint equation, has also been tested in Phase I. It is less computationally intensive (due to the avoidance of log-calls and the need for a Newton-Raphson root finder at each spatial node and time iteration) and shorter wallclock time than the ELB-Q27 code, see Table I.

V. QUANTUM INFORMATION PROCESSING

Quantum information processing (QIP) and quantum communications will be integral to the 21st century. For many years, QIP has been included in the Developing

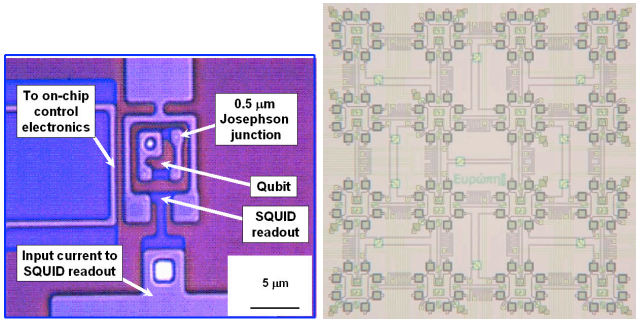

FIG. 5: Shown here is a newsworthy achievement of a first quantum information processor circuit to embody a qubit (left), a basic device for storing quantum information, designed by Terry Orlando of MIT and build at MIT Lincoln Laboratory at Hanscom AFB in 2000 [6, 7]. The circuit must be placed in a dilution refrigerator. Air Force Office of Scientific Research (AFOSR) supported novel quantum computing technology based on superconductive electronics under the Quantum Computation for Physical Modeling (QCPM) theme, and this research has recently found follow-on use. A superconducting wire loop with multiple Josephson junctions forms a qubit and such qubits are coupled together to make quantum logic gates. AFOSR funded this new solid-state technology, fabricated at the superconductive electronics foundry at MIT Lincoln laboratory. This helped establish the basic fabrication techniques to build scalable quantum computers and mapped the quantum control methodology, proven with NMR spectroscopy [4, 5], onto the field of superconductive electronics for quantum information processing, mapping pulse protocols to allow qubit-qubit logical operations, constituting a basic 2-qubit quantum processor. Going from a 2-qubit processor to a 16-qubit processor necessarily entails a significant applied research effort recently announced by D-Wave, a Canadian start-up company. D-Wave's 16-qubit processor, fabricated by NASA, is shown (right).

Science and Technologies List, in the section of critical information systems technology. There now exists the possibility of the development of large quantum computer arrays, potentially outstripping any supercomputers now used for defense department computations.

On Babbage Q27, Q19, Q15 lattice Boltzmann codes were tested, like the one shown in Figure 1. Using 2,048 processors it took two days to complete a single job. A $1,024^3$ grid takes about 44 hours for Q27 on 512 processors, while the corresponding run for Q15 takes about 28 hours. The cost of the largest supercomputer parallel arrays annually adds to a significant fraction of a billion dollars for new government-owned systems in the United States (*e.g.* 19,000 processor Franklin at DOE/NERSC cost about $50 million and occupies the space of a gymnasium). Remarkably, exploiting quantum mechanical complexity new quantum device technology can be used to efficiently compute the collision operator of the Q15 lattice Boltzmann code, the basic engine of the code.

Therefore, a relatively low cost and small type-II quantum computer with a few thousand 16-qubit quantum processor chips, perhaps cooled with dilution refrigeration, could handle the same supercomputing job. It could cost a few million dollars to assemble, a couple orders of magnitude less expensive than classical digital electronics based supercomputers, such as Babbage, and physically smaller by many orders of magnitude as well. Furthermore, future quantum processor arrays with more qubits per node, if available in the near future, could outstrip any traditional parallel supercomputer purchased under the department of defense high performance computing modernization program.

The kinetic lattice gas model has proven to be a state-of-the-art tool for understanding the morphological evolution of turbulence.

VI. ACKNOWLEDGEMENTS

This work was supported in part by a grant of computer time from the defense department High Performance Computing Modernization Program, with computational support from the Major Shared Resource Centers: the Naval Oceanographic Office and the US Army Engineer Research and Development Center. JY would like to acknowledge the leaders in the Air Force Office of Scientific Research. The AFOSR Novel Strategies for Parallel Computing Initiative launched in 1992, and two subsequent AFOSR quantum computing research projects launched in 1996 and 2000, allowed us to lay a firm foundation theoretically, experimentally, and numerically for this lattice model of turbulence suited for both parallel supercomputers and quantum computers.

Appendix A: Mathematical formulation

In the lattice model, dynamics is projected into a discrete kinetic phase space. The logical "1" state (the excited state) of a qubit $|q\rangle$ associated with the spacetime point $(\vec{x}, t)$ encodes the probability f_q of the existence of a particle at that point moving with velocity $\vec{c}_q = \frac{\Delta\vec{x}_q}{\Delta t}$, where $\Delta\vec{x}_q$ are lattice vectors, for $q = 1, 2, \ldots, Q$. A fundamental property of the lattice model is that particle motions in momentum space and position space occur independently [8]. Particle momentum and position space motions are generated by the combination of an engineered qubit-qubit interaction Hamiltonian H' and a free Hamiltonian $-i\hbar\sum_q \vec{c}_q \cdot \nabla$, respectively.

All the particle-particle interactions, the 2-body up to and including all the $(Q-2)$-body interactions, generated by H' are mapped to a local collision function $H' \mapsto \Omega_q$ that depends on all the f_q's at the lattice site [3].

In the type-II quantum computing case, quantum entanglement is localized among qubits associated with the same $(\vec{x}, t)$ [9], so:

$$f'_q(\vec{x}, t) = f_q(\vec{x}, t) + \Omega_q(f_1, f_2, \ldots f_Q) \quad \text{(A1a)}$$

$$f_q(\vec{x}, t) = f'_q(\vec{x} - \Delta\vec{x}_q, t - \Delta t), \quad \text{(A1b)}$$

where f_q and f'_q are called the *incoming* and *outgoing* probabilities, respectively. In the classical limit, there

exists a fundamental entropy function

$$\mathscr{H}(f_1,\ldots,f_Q)=\sum_{q=1}^{Q} f_q \ln(\gamma_q f_q), \qquad \text{(A2)}$$

where the γ_q are self-consistently determined positive weights ($\sum_q \gamma_q = 1$). Ω_q in (A1a) is determined by the constant entropy condition:

$$\mathscr{H}(f'_1,\ldots,f'_Q)=\mathscr{H}(f_1,\ldots,f_Q). \qquad \text{(A3)}$$

It is (A1) through (A3) that constitutes the lattice model of fluid turbulence suited for parallel supercomputers.

In the Q-dimensional kinetic space, the equilibrium distribution $f_q^{\rm eq}$, taken as a vector, is the bisector of the difference of the incoming and outgoing kinetic vectors:

$$f_q \;=\; f_q^{\rm eq}-\frac{1}{\alpha\beta}\Omega_q \qquad f'_q=f_q^{\rm eq}+\left(1-\frac{1}{\alpha\beta}\right)\Omega_q, \text{(A4a)}$$

when $\lim_{\eta\to 0}\alpha\beta = 2$ and where $f_q^{\rm eq}$ is analytically determined by extremizing (A3) subject to the two constraints of conversation of probability and probability flux. Eliminating Ω_q from (A4) yields an operative collision equation simpler than (A1a)

$$f'_q = f_q + \alpha\beta\left(f_q^{\rm eq}-f_q\right). \qquad \text{(A5)}$$

Finally, eliminating f'_q in (A1b) and (A5), yields the lattice Boltzmann equation

$$f_q(\vec{x}+\Delta\vec{x}_q,t+\Delta t)=f_q(\vec{x},t)+\alpha\beta\left[f_q^{\rm eq}(\vec{x},t)-f_q(\vec{x},t)\right], \qquad \text{(A6)}$$

in the BGK collisional limit [10]. Since $\alpha\beta$ and $f_q^{\rm eq}$ are determined by (A2), (A6) is called the *entropic lattice Boltzmann equation* [11].

The kinetic lattice gas model becomes equivalent to the Navier Stokes equations:

$$\partial_t\vec{u}+\vec{u}\cdot\nabla\vec{u}=-\nabla P+\eta\nabla^2\vec{u} \qquad \text{and} \qquad \nabla\cdot\vec{u}=0, \quad \text{(A7)}$$

where $\vec{u}=\vec{u}(\vec{x},t)$ is the vectorial flow field, where the pressure is proportional to the field density ($P=\rho c_s^2$, with spatial dimension D and sound speed $c_s=\frac{1}{\sqrt{D}}\frac{\Delta r}{\Delta t}$), and where the shear viscosity is the measure of dissipation (a renormalized transport coefficient for momentum diffusion). In the limit when $\Delta\vec{r}\to 0$ and $\Delta t\to 0$ and the hydrodynamic variables are cast as moments of the probability distribution, $(\rho c,\vec{u})=\sum_q (c,\vec{c}_q) f_q$ [12]. The hydrodynamic variables are independently evaluated at each spacetime point $(\vec{x},t)$. The shear viscosity is analytically determined, and the result is

$$\eta=\rho c_s^2\Delta t\left(\frac{1}{\alpha\beta}-\frac{1}{2}\right), \qquad \text{(A8)}$$

so the model approaches the inviscid limit where $\eta\to 0$ as $\alpha\beta\to 2$ [13].

[1] S. A. Orszag and G. S. Patterson. *Statistical Models and Turbulence*. Springer-Verlag, New York, 1972. editors M. Rosenblatt and C. Van Atta.

[2] S. Kida and Y. Murakami. Kolmogorov similarity in freely decaying turbulence. *Physics of Fluids*, 30(7):2030–2039, 1987.

[3] Jeffrey Yepez. Quantum lattice-gas model for computational fluid dynamics. *Physical Review E*, 63(4):046702, Mar 2001.

[4] Marco Pravia, Zhiying Chen, Jeffrey Yepez, and David G. Cory. Towards an NMR implementation of a quantum lattice gas algorithm. *Computer Physics Communications*, 146(3):339–344, 2002.

[5] Zhiying Chen, Jeffrey Yepez, and David G. Cory. Simulation of the Burgers equation by NMR quantum-information processing. *Physical Review A*, 74(4):042321, Oct 2006.

[6] J.E. Mooij, Terry P. Orlando, L. Levitov, Lin Tian, Casper H. van der Wal, and Seth Lloyd. Josephson persistent-current qubit. *Science*, 285:1036–1039, 1999.

[7] T.P. Orlando, J.E. Mooij, Lin Tian, Caspar H. van der Wal, L.S. Levitov, Seth Lloyd, and J.J. Mazo. Superconducting persistent-current qubit. *Physical Review B*, 60(22):15398–15413, 1999.

[8] Jeffrey Yepez. Relativistic path integral as a lattice-based quantum algorithm. *Quantum Information Processing*, 4(6):471–509, Dec 2005.

[9] Jeffrey Yepez. Open quantum system model of the one-dimensional Burgers equation with tunable shear viscosity. *Physical Review A*, 74(4):042322, Oct 2006.

[10] P. L. Bhatnagar, E. P. Gross, and M. Krook. A model for collision processes in gases. i. small amplitude processes in charged and neutral one-component systems. *Phys. Rev.*, 94(3):511–525, May 1954.

[11] Bruce M. Boghosian, Jeffrey Yepez, Peter Coveney, and Alexander Wagner. Entropic lattice Boltzmann methods. *Proceedings of the Royal Society A: Mathematical, Physical and Engineering Sciences*, 457(2007):717–766, Mar 2001.

[12] Bruce M. Boghosian, Peter J. Love, Peter V. Coveney, Iliya V. Karlin, Sauro Succi, and Jeffrey Yepez. Galilean-invariant lattice-Boltzmann models with H theorem. *Physical Review E*, 68(2):025103, Aug 2003.

[13] Brian Keating, George Vahala, Jeffrey Yepez, Min Soe, and Linda Vahala. Entropic lattice Boltzmann representations required to recover navier-stokes flows. *Physical Review E*, 75(3):036712, 2007.